Distinct Functional and Structural Neural Underpinnings of Working Memory

Max M. Owens[a], **Bryant Duda**[a], **Lawrence H. Sweet**[a,b], **James MacKillop**[c,d,a]

[a]Department of Psychology, University of Georgia, 125 Baldwin Street, Athens, GA 30602

[b]Department of Psychiatry and Human Behavior, Brown University, Box G-A1, Providence, Rhode Island 02912

[c]Peter Boris Centre for Addiction Research, St. Joseph's Healthcare Hamilton/ McMaster University, 100 West 5th Street, Hamilton, ON L8P 3R2, Canada

[d]Homewood Research Institute, 150 Delhi Street, Riverslea Building, Guelph, ON N1E 6K9 Canada

SUMMARY

Working memory (WM), the short-term abstraction and manipulation of information, is an essential neurocognitive process in daily functioning. Few studies have concurrently examined the functional and structural neural correlates of WM and the current study did so to characterize both overlapping and unique associations. Participants were a large sample of adults from the Human Connectome Project (*N*=1064; 54% female) who completed an in-scanner visual N-back WM task. The results indicate a clear dissociation between BOLD activation during the WM task and brain structure in relation to performance. In particular, while activation in the middle frontal gyrus was positively associated with WM performance, cortical thickness in this region was inversely associated with performance. Additional unique associations with WM were BOLD activation in superior parietal lobule, cingulate, and fusiform gyrus and gray matter volume in the orbitofrontal cortex and cuneus. Across findings, substantially larger effects were observed for functional associations relative to structural associations. These results provide further evidence implicating frontoparietal subunits of the brain in WM. Moreover, these findings reveal the distinct, and in some cases opposing, roles of brain structure and neural activation in WM, highlighting the lack of homology between structure and function in relation to cognition.

Keywords

Working memory; structural MRI; functional MRI; N-Back

Corresponding Author: James MacKillop, PhD, Peter Boris Centre for Addictions Research, St. Joseph's Healthcare Hamilton, West 5th Campus/McMaster University, 100 West 5th Street, Hamilton, ON L8P 3R2, Canada, jmackill@mcmaster.ca.

INTRODUCTION

Working memory (WM) refers to the brain's capacity for short-term abstraction and manipulation of information, its "scratchpad," and it is an essential neurocognitive process in in diverse aspects of daily functioning. Furthermore, deficits in WM performance have been associated with a variety of psychiatric and neurological disorders, including attention deficit hyperactivity disorder (Martinussen et al., 2005), schizophrenia (Goldman-Rakic, 1994; Silver et al., 2003), multiple sclerosis (Bobholz and Rao, 2003; Rao et al., 1993), and addiction (Bickel et al., 2011). In terms of the neural substrates of WM, functional magnetic resonance imaging (fMRI) studies have revealed a bilateral network comprising dorsolateral prefrontal cortex, inferior parietal lobule, supplementary motor area, ventrolateral prefrontal cortex, and premotor cortex (Owen et al., 2005; Yeo et al., 2015). This putatively reflects the executive control network (ECN), which is implicated in diverse executive functions including working memory (Niendam et al., 2012). Supporting this, greater ECN activity has been associated with better WM performance (Burgess et al., 2011; Cabeza et al., 2002; Chein et al., 2011; Nyberg et al., 2009; Osaka et al., 2004) and WM training improves both WM performance and ECN activity (Olesen et al., 2004).

A second bilateral network has been repeatedly shown to be inversely related (less active) to WM performance (McKiernan et al., 2003; Sweet et al., 2008). The regions in this network include ventromedial prefrontal cortex, posterior cingulate cortex, angular gyrus, and lateral and medial temporal cortex. Collectively, these regions have been referred to as the default mode network (DMN), the resting state network, and the task-negative network (Andrews-Hanna et al., 2010; Buckner et al., 2008), all putatively reflecting passive cognitive activity at rest and unengaged in a cognitive task. As a result, suppression of DMN is considered an index of cognitive effort.

While most WM paradigms use verbally encoded stimuli (such as letters or number) held in working memory in a phonological loop, it is also common for paradigms to use visually encoded stimuli (Owen et al., 2005; Wager and Smith, 2003). While there have been some differences found between verbal and visual working memory, these differences are relatively minor and there is no agreed upon interpretation. For example, one review found evidence suggesting that verbal working memory is lateralized more so in the left hemisphere and visual WM more so in the right hemisphere (Wager and Smith, 2003). This has been suggested may be due to the left hemisphere's unique role in language and the right hemisphere's role in spatial skills, as evidenced in case studies of lesions to these hemispheres (Smith and Jonides, 1997), but this idea is still controversial. However, meta-analyses have revealed that although there may be differences (e.g., spatial WM may be more right lateralized), if they exist they are of small magnitude and the general networks implicated in verbal and visual working memory are very similar (Owen et al., 2005; Wager and Smith, 2003).

In contrast to extensive functional magnetic resonance imaging (fMRI) findings, relatively few studies have examined the morphometric (structural) correlates of WM and no meta-analyses or systematic reviews have been conducted on the topic to date. In a recent

example, in healthy older adults (N=56) greater gray matter in medial orbitofrontal cortex, inferior frontal gyrus, and superior frontal gyrus were found to be associated with WM performance (Nissim et al., 2017). These findings and a small number of other structural studies (Salat et al., 2002; Takeuchi et al., 2011) have been generally interpreted as being consistent with the fMRI findings. However, this may be partially because the functional findings served as the basis for identifying regions of interest in the structural studies. The small number of studies in this area may be a function of small effect size relationships that require large samples to detect statistically significant associations.

Even fewer studies have directly tested whether the association of brain activation during WM tasks relates to brain structure. In the only study to do so to date, cortical thickness was not associated with brain activation during a visual WM task in any region of the brain (Squeglia et al., 2013). In regions which were expected to show strong structure/function relationships such as the anterior cingulate, orbitofrontal cortex, middle frontal gyrus, superior parietal lobule, Pearson correlations were less than .10 and in no region were they greater than .18. No associations of structure and function were significant beyond multiple comparison correction. Furthermore, no studies have tested whether the previously described associations of brain function and structure to WM performance are describing the same process (i.e., one is dependent on the other) or contributing to WM performance in unique ways (i.e., they are orthogonal).

The current study sought to advance the understanding of the neural correlates of WM and to further address the question of overlap, concurrently examining functional and structural correlates of WM to characterize the common and unique underpinnings of this critical cognitive process. To do so, the investigation leveraged data from the Human Connectome Project, a large multi-modal open-science project that includes over 1200 participants (Van Essen et al., 2013a). Based on the sizable fMRI literature, WM processing was predicted to recruit neural activity in subunits of the ECN, but specific structural predictions were not made based on the inconsistency in findings. Based on the work of Squeglia et al. (2013), we expected to find a dissociation between brain structure and function such that regional brain activation displayed while engaging in a WM task would relate differently to WM performance than regional brain structure (i.e., different regions would predict WM performance in functional and structural MRI analyses). In order to test these hypotheses, the current study used Blood Oxygen Level Dependent (BOLD) fMRI activation and high resolution structural MRI during a visual N-back WM task. The N-back task comprises sequences of stimuli that participants evaluate for the presence of a stimulus, n items ago (i.e., participants are required to hold previous stimuli in mind and compare them to the test stimuli). In this case, participants were presented with images of places, tools, faces, and body parts. During a control task (the 0-back), participants were presented with a target cue and then instructed to identify any stimuli that matched the target; during the WM task (the 2-back), participants were required to identify stimuli that matched the stimulus presented two trials prior (full details in Online Methods). The N-Back is one of the most commonly used WM paradigms, although it is not interchangeable with other measures of WM (Redick & Lindsey, 2013). The functional MRI index was blood-oxygenation-level-dependent (BOLD) activity for the contrast between the 2-back and 0-back in relation to behavioral performance. For structural MRI indices, gray matter volume (GMV) and cortical thickness

were examined throughout the cortex for association with WM performance accuracy (2-back accuracy), as well as accuracy on the 0-back to help parse what elements of the brain/behavior relationship detected for the 2-back can be attributed to simple visual attention. Both GMV and cortical thickness were examined because the two are largely uncorrelated and both have been used in the prior WM structural literature. Both structural and functional data were analyzed using both brain atlas-based regions (Desikan et al., 2006) as the primary focus of the study, as it would allow for easier integration of structural and functional results and the comparison of effect sizes between the two sets of findings. Voxelwise analyses were included to complement the atlas-based results and verify that the findings were not an artifact of idiosyncrasies of the atlas. Last, integrative analyses of both structure and function from the atlas-based analyses were completed to identify convergence and divergence between structural and functional imaging modalities and to characterize their combined relationship to WM performance.

RESULTS

Associations of Working Memory Performance with Brain Function

Across atlas-based and voxelwise analyses, common regions in the executive control and default mode networks were associated with 2-back accuracy. Following FDR correction, partial correlations indicated significant positive associations between BOLD activation and 2-back accuracy in a number of regions of the executive control network (e.g., middle frontal gyrus, posterior parietal cortex) and negative associations with regions of the default mode network (e.g., medial orbitofrontal cortex, isthmus of the cingulate cortex; significant associations in Table 2A, all associations in Supplementary Table 3). From the voxelwise analyses, similar clusters were indicated in which activation was significantly associated with 2-back accuracy at $p < $ 1E-11 with a cluster size threshold of 200 voxels, including positive associations in the middle frontal gyrus, posterior parietal cortex, supplementary motor area and negative associations in the medial orbitofrontal cortex and posterior cingulate cortex (results shown in Table 2B and Figure 3).

Associations of Working Memory Performance with Brain Structure

For GMV, partial correlations incorporating age indicated that 2-back accuracy was positively associated with total cortical GMV ($r = .092$, $p = .003$; Supplementary Figure 1). For the Desikan atlas regions, significant partial correlations with 2-back accuracy, following FDR correction, are in Table 1A (all associations are in Supplementary Table 1). The largest associations were for bilateral orbitofrontal cortex, cuneus, and middle temporal gyrus. For the voxelwise analyses, clusters in which GMV was significantly associated with 2-back accuracy at clusterwise $p < .05$ are in Table 1B and Figure 1. The results largely converged with the atlas-based findings, with common regions including bilateral lateral orbitofrontal cortex, left cuneus, right middle temporal gyrus, right pars orbitalis and left inferior temporal gyrus.

For regional cortical thickness, in partial correlation analyses using the 68 regions of the Desikan atlas, only the left ($r = -.148$, $p = $ 1.1E-6) and right ($r = -.102$, $p = .001$) caudal middle frontal gyrus and the left frontal pole ($r = -.096$, $p = .002$) were associated with 2-

back accuracy beyond FDR correction. All partial correlations for thickness are in Supplementary Table 2. Consistent with this, the voxelwise analyses revealed two significant regions (clusterwise $p < .05$), an inverse association with left caudal middle frontal gyrus (size: 767 mm^3; coordinates: x = −36, y= 16, z = 51; CWP = .0002) and a positive association was present between 2-Back performance and right temporal pole (size: 288 mm^3; coordinates: x = 30, y = 3, z = −31; CWP = .0042) (Figure 2).

Integration of Structural and Functional Findings

The integrative regression model (Table 3) accounted for 26.5% of the total variance in 2-back accuracy. In this model, regions whose GMV, thickness, or BOLD activity was bilaterally associated with 2-back accuracy were consolidated to limit issues of multicollinearity (see Online Methods and Supplementary Table 4 for details). Collectively, the integrative analysis revealed unique contributions of greater activation in several ECN regions (middle frontal gyrus, posterior parietal cortex) greater deactivation in DMN regions (medial orbitofrontal cortex, inferior parietal lobule), greater GMV in bilateral lateral orbitofrontal cortex and cuneus, and reduced cortical thickness in caudal middle frontal gyrus.

Last, the associations between corresponding Desikan atlas regions of brain structure and function were directly investigated. For GMV, using an FDR correction, significant associations with BOLD activation were present in 12 regions (Table 4). However, the associations were mixed in direction (i.e., greater GMV was not consistently associated with greater BOLD signal) and they were uniformly small in magnitude, accounting for 0.6% to 2% of shared variance. In addition, of the significantly associated indices, only a subset overlapped with those found to be significantly associated with 2-back accuracy. For cortical thickness, no correlations with BOLD activation were significant. Collectively, atlas-based associations between BOLD signal and morphometry suggested minimal overlap of structure and function in relation to 2-Back performance. All structure/function correlations are in Supplementary Tables 5 and 6.

DISCUSSION

This study used multiple complementary strategies to systematically characterize the functional and structural neural correlates of WM and to test the hypothesis that there would be a substantial dissociation between the two modalities. To do this, the current study concurrently characterized BOLD signal, GMV, and cortical thickness in relation to a 2-back task and then integrated these indices and examined their interrelationships.

Consistent with predictions, the functional results indicating the ECN and DMN were activated during WM and their activation was related to WM performance were in expected regions (e.g., dorsolateral prefrontal cortex, posterior parietal cortex) based on prior literature (Burgess et al., 2011; Cabeza et al., 2002; Chein et al., 2011; Nyberg et al., 2009; Osaka et al., 2004; Owen et al., 2005; Sweet et al., 2008). However, the structural results indicated effects in regions not previously reported to be associated with WM, such as effects for GMV in the lateral orbitofrontal cortex, cuneus, and the lateral temporal lobe. An exception to this was cortical thickness in the middle frontal gyrus, for which there is prior

evidence that this region is a central node in the ECN (Miller, 2000; Niendam et al., 2012) and greater functional activity is associated with better working memory, cognitive flexibility, vigilance, and future planning (Niendam et al., 2012). There is also evidence suggesting specifically that thinner middle frontal gyrus is associated with better WM performance (Takeuchi et al., 2011). This presumably reflects increasing efficiency of deployment as cortical thinning is in this region occurs throughout adolescence and early adulthood as part of normal development and is linked to improved executive functioning (Herting et al., 2015; Lemaitre et al., 2012; Vijayakumar et al., 2016). In the current findings, thinner and more active middle frontal gyri were uniquely predictive of WM performance.

There is some previous evidence linking greater GMV in the lateral orbitofrontal cortex to WM performance (Salat et al., 2002) and the ventrolateral PFC is considered a part of the ECN as well (Niendam et al., 2012; Osaka et al., 2004). However, some other implicated regions have no empirical precedent. For example, this is the first study to link cuneus GMV to WM performance. The cuneus is typically understood to subserve basic visual processing (Vanni et al., 2001), though there is also evidence that it may play a role in response inhibition (Haldane et al., 2008). Given the association of both the orbitofrontal cortex and cuneus with behavioral inhibition, it is possible that greater structural integrity in these regions could relate to WM by preventing premature responding. Alternatively, the visual nature of this N-Back task may be the reason the cuneus was robustly implicated. Because the N-back task elicits numerous cognitive processes in addition to working memory and structural MRI analysis doesn't use a contrast approach (as is used in fMRI), it is difficult to definitively determine the role of the structure of these regions from the current data. However, when the current analyses were repeated with 0-back accuracy, relationships were found between 0-back accuracy and GMV in a different set of regions (bilateral temporal pole, right entorhinal cortex) and 0-back accuracy was unrelated to cortical thickness in any regions (0-back associations in Supplemental Tables 7 and 8). Specifically, GMV in the cuneus was related to 2-back accuracy only and not 0-back accuracy. These findings provide some evidence that the regions whose structure was implicated in the current results may be uniquely relevant to the WM processes occurring in the N-back, but do not provide definitive proof of this.

Beyond the individual associations, important collateral findings pertain to differences in the magnitudes of effects and evidence of dissociation between structure and function. In the functional imaging results, ECN engagement and DMN disengagement were associated with WM performance with a large combined effect size (largest individual effect size $r = .32$ and combined $R^2 = .17$ in hierarchical regression). In the structural imaging results, GMV in the lateral orbitofrontal cortex and the cuneus were positively associated with WM performance and cortical thickness in the caudal middle frontal gyrus was inversely associated with WM performance and the effect sizes of these associations were much smaller (largest individual effect size $r = .12$ and combined $R^2 = .02$ beyond functional associations). Particularly salient dissociations between structure and function were present for middle frontal gyrus (a positive functional association but a negative structural relationship) and subunits of orbitofrontal cortex (negative functional association for medial orbitofrontal cortex, but a positive structural association for lateral orbitofrontal cortex).

Finally, when directly compared, the structural and functional indices were largely orthogonal, with each contributing unique variance to the prediction of WM performance, no associations between cortical thickness and activation, and inconsistent associations between the GMV and activation.

Another significant finding in the current study pertains to how brain structure and function relate to each other and have implications beyond WM. That cortical activation and cortical structure were orthogonally related to WM performance, and were only selectively related to each other directly, contradicts a common (and often unstated) assumption of cognitive neuroscience that in regions whose activation relates to a task, a similar relationship should be expected regarding brain structure. In practice, this means that studies attempting to investigate cognitive processes via structural MRI should not use the functional neuroimaging literature as a default template for selecting regions of interest, as is common (Almeida et al., 2010; Bjork et al., 2009; Durazzo et al., 2011; Raine et al., 2000; Yang et al., 2005), and should not over interpret findings based on their close or distant alignment with the functional literature (and vice versa). Rather, neuroimaging studies should focus on investigating the brain within a given modality and minimize assumptions about commonalities across modalities.

A second broad implication was the extent to which these neuroimaging methods were linked to behavioral output. Given how much larger effect sizes were for WM performance's association with BOLD activations than with GMV or cortical thickness, the current results suggest that neural activation is a much more proximal index of cognitive ability than brain structure. While this is not the first finding suggestive of this difference (Squeglia et al., 2013), it crystalizes this sentiment by showing substantial differences in effect size for brain/behavior relationships using MRI and fMRI in the same large sample. This naturally raises questions about the clinical significance of the structural findings, which accounted for less than 2% of the variance in WM performance. While the large sample size and very high levels of statistical significance suggests these results would likely replicate, it is certainly debatable the real-world value of a measure with such little predictive power.

Finally, although the large sample brought the findings from both modalities into sharp relief and revealed distinct neural underpinnings, it is also worth noting that despite thoroughly exploring BOLD activation, GMV, and cortical thickness, the final model including BOLD signal, GMV, and cortical thickness explained only 26% of the variance in WM performance (of which about 7% was explained by covariates). Since logically all cognition is traceable to the brain at some level, this suggests that there is substantial variation in performance that remains to be explained by other neuroimaging methods. Of course, the prediction of 100% of behavioral performance will never be possible because of measurement error, but these findings nonetheless highlight that commonly used measures of structure and functional only captured a minority of the variation.

Of note, several considerations bear on the present findings. First, it is important to note that that these results may not extend to all WM tasks. For example, N-Back accuracy has exhibited only modest associations with digit span as a measure of WM (Kane et al., 2007) (Jacola et al., 2014). Similarly, a recent meta-analysis found that N-back accuracy was only

weakly correlated to span tests of WM, with substantial variation across the literature (Redick and Lindsey, 2013). Other studies have found that N-back accuracy relates more strongly to measures of processing speed (Miller et al., 2009) or fluid intelligence (Jaeggi et al., 2010) than to other measures of WM. One possible reconciliation of these findings is increasing evidence that WM is not a unitary construct, as it was originally conceptualized, but a complex cognitive process with multiple and independent elements such as encoding, recall, maintenance, updating, ordering, attention, and inhibition (Oberauer et al., 2012; Redick and Lindsey, 2013; Unsworth et al., 2009). Overall, this literature suggests that caution should be taken in extrapolating the current results to other WM tasks and indeed that there may closer parallels to tasks measuring other related cognitive processes. A related consideration was that the study used a pictorial N-back, testing visual WM rather than verbal WM. However, while the verbal N-back is the more commonly used form of the task, meta-analytic findings suggest that both versions of the task generally elicit the same networks of activity (Owen et al., 2005). Additionally, while some have suggested that visual working memory tasks would be more right lateralized than verbal tasks (Smith and Jonides, 1997; Wager and Smith, 2003), we found no clear evidence of results favoring the right hemisphere in the current study. Another methodological note is that the sample was relatively young adults, 22–35 and was intentionally comprised of generally healthy subjects. Thus, the generalizability of these findings to other age groups or to individuals with psychiatric or neurodegenerative diseases is not clear.

A second broad consideration is the decision to approach the current study from an exploratory whole-brain perspective (rather than an *a priori* region of interest perspective), which was made intentionally for maximal scope and to avoid making assumptions. Given that the largest study to date to test the relation of brain activation during WM to brain structure found no associations between structure and function across the entire brain in 156 participants (Squeglia et al., 2013), we thought it was essential to test the associations of brain structure and function with WM performance and each other across the entire brain, rather than only in specific regions. Another important consideration is the differences in the ability of structural and functional analysis to isolate elements of the N-back task pertaining to WM specifically. fMRI analysis uses contrasts which allow for an active baseline to be used in order to subtract out elements of activation relating to cognitive processes of non-interest (such as visual activation from viewing a screen or motor activation from pressing a button with the finger) leaving only the process of interest (in this case, WM). On the other hand, brain structure is measured in an absolute scale (e.g., cortical thickness of 2 mm) and independent of the task itself. Consequently, statistical association of WM task performance with brain structure does not isolate WM elements of the task, meaning structural results also include elements of visual processing, motor response, etc. To partially respond to this issue, we report the relation of performance on the visuomotor control task (the 0-back) with brain structure as well, demonstrating different regional associations from the primary WM task. This provides some evidence that the current results are specifically related to the WM processes in the 2-back rather than other cognitive processes necessary to completing the task.

With these considerations in mind, the current study nonetheless provides strong evidence for the specific functional and structural brain regions implicated in working memory,

dissociation between brain structure and function, and evidence of substantially larger effect sizes relationships for functional activity. In particular, robust increases in BOLD activation in subunits of the ECN and decreases in activation in the DMN were associated with better WM performance, whereas, structurally, higher GMV in the orbitofrontal cortex and lower cortical thickness in the middle frontal gyrus were associated with better WM performance. Given its large sample size and atlas-wide scope, these findings suggest that similar dissociations are likely to exist for other and, perhaps most, cognitive processes. Given little evidence of homology, caution is warranted when extending findings from one imaging modality to another.

METHODS

Participants

As part of the HCP (http://www.humanconnectome.org/), MRI and N-back WM task data were collected from 1064 participants at Washington University in St. Louis over the course of two days between August 2012 and October 2015, and released in full on March 1, 2017. Informed consent was obtained for all participants using the procedure detailed in Van Essen et al (D. C. Van Essen et al., 2013). Participants were 22–35 years old and had no significant history of neurological disorder or damage, cardiovascular disease, Mendelian genetic disease (e.g., cystic fibrosis), or MRI contraindications, such as metal devices in the body or claustrophobia. For demographics characteristics of the current sample see Table 5 and for full details of inclusion and exclusion criteria, see van Essen et al. (D. Van Essen et al., 2013).

N-back Task

WM performance was investigated using N-back fMRI paradigm in which participants were presented with blocks of trials that consisted of places, tools, faces, and body parts. Within each run, the 4 different stimulus types were presented in separate blocks. Each of two runs contained 8 N-back task blocks (27.5 sec each), consisting of four 0-back blocks and four 2-back blocks, and four resting/eye fixation blocks (15 sec each). A 2.5 sec cue was presented at the beginning of each block to inform participants which task followed (i.e., 0-back or 2-back), 10 trials of 2.5 sec each were included in each block. On each trial, the stimulus was presented for 2 sec, followed by a 500 ms inter-trial interval. During 0-back task blocks, participants were presented with a target cue and then instructed to identify any stimuli that matched the target. During 2-back task blocks, the subject was required to identify stimuli that matched the stimulus presented two trials prior.

MRI Data Acquisition

High-resolution structural images were collected on a 3T Siemens Skyra scanner (Siemens AG, Erlanger, Germany) with a 32-channel head coil. T1-weighted structural images were acquired with a resolution of 0.7 mm^3 isotropic (FOV = 224×240, matrix = 320×320, 256 sagittal slices; TR = 2400 ms and TE = 2.14 ms). Morphometric analyses were completed using FreeSurfer Image Analysis Suite version 5.3 (http://surfer.nmr.mgh.harvard.edu; Fischl, 2012) following preprocessing using Freesurfer's standard recon-all pipeline function (Fischl et al., 2001, 1999b) and using Rorden's DICOM to NIFTI conversion software

(Rorden, 2007). For details of acquisition parameters, reconstruction, and preprocessing of the Human Connectome Project structural MRI data, see van Essen et al. and Glasser et al. (Glasser et al., 2013; D. Van Essen et al., 2013). All structural images were reviewed by a technician immediately following acquisition to ensure scans did not have any significant problems (i.e., artifacts, substantial movement). If problems were found, structural scans were reacquired immediately. Within hours of the initial acquisition, scans were examined by quality control specialists who assessed them for blurriness, motion and other artifacts. Based on these factors, scans were rated on a 1 to 4 scale (poor to excellent). In all cases where structural scans were below 3 (good), new structural scans were reacquired on the participant's second study day. Through this process, high quality structural imaging data was acquired from all participants. For a full explanation of the HCP quality control parameters, see Marcus et al. (Marcus et al., 2013).

fMRI data were collected during the N-back paradigm using a 32-channel head coil on a 3T Siemens Skyra. Two 5:01 runs of the task were completed using the following acquisition parameters: TR = 720 ms, TE = 33.1 ms, flip angle = 52 degrees, FOV = 208 × 180 mm, 72 2mm-thick sagittal slices, 2.0mm isotropic voxels. A multi-band acceleration factor of 8 was used. One imaging run was acquired left to right, and the other was acquired right to left. Data were preprocessed by HCP scientists using the minimal preprocessing pipeline (Glasser et al., 2013) that includes gradient unwarping, motion correction, field-map based EPI distortion correction, brain boundary-based registration of EPI to the structural scan, registration into MNI152 space, and grand-mean intensity normalization.

Data Analysis

Working Memory Performance and Functional Activation during Working Memory Task—fMRI data was downloaded having been preprocessed by the minimal preprocessing pipeline described above (Glasser et al., 2013). Additional fMRI data processing and analysis were then conducted using the Analysis of Functional NeuroImages software (AFNI; Cox, 1996) Data were spatially smoothed using a 6mm full width half maximum Gaussian filter. General linear modeling was completed using regressors for blocks of each condition (2-back, 0-back, and instruction screens), six nuisance regressors to account for motion (x, y, z, roll, pitch, yaw), and regressors for linear, quadratic, and cubic trends. The measure of WM performance in these analyses was accuracy on the 2-back, which was tested for its association with functional activation while participants completed the 2-back task. We also considered also using d', a signal detection theory approach to evaluate WM performance, but it was collinear with 2-back accuracy ($r = .96$). Given its redundancy and the fact that it is less intuitively interpretable than performance accuracy, it was not included. Activation during 2-back was measured against a baseline of activation during the 0-back task, which is matched on most visual/behavioral/cognitive characteristics (except WM demands) and is effectively a task of sustained attention. To provide a direct comparison to the structural findings, the average activation for each subject the 64 (out of 68) regions of the Desikan atlas able to be mapped in the space of the functional data during 2-back (relative to 0-back) was extracted to SPSS using 3dROIstats (note that right and left pericalcarine fissure and right and left banks of the superior temporal sulcus could not be extracted due to differences in functional and structural mapping of the Desikan atlas).

Consistent with the GMV and cortical thickness analyses, activation in each of these regions was then tested for association with 2-back accuracy using partial correlation with a two-tailed false discovery rate correction (Benjamini and Hochberg, 1995) of $q = .05$ to reduce inflation of type I error rate. To provide an whole-brain approach analogous to the voxelwise cortical surface analysis conducted on GMV and cortical thickness (see below), a voxelwise correlation of brain activation during 2-back (relative to 0-back) with 2-back accuracy was completed using the covariate feature of the AFNI program 3dttest++. To correct for family wise error, a threshold of $p < 1E-11$ was used with a cluster size threshold of 200 voxels. This threshold was substantially more stringent than a cluster-corrected threshold of $p < .05$ and was selected because, given the large number of subjects and high-magnitude brain activation, a standard threshold did not differentiate meaningful clusters (i.e., almost the entire brain was positively or negatively associated with 2-back accuracy at a standard threshold).

Working Memory Performance and Gray Matter Volume/Cortical Thickness—
The behavioral measure of WM performance used was accuracy on the 2-back task. Age and total intracranial volume (ICV) were used as covariates in all analyses. These covariates were chosen due to their potentially confounding relationship with WM function and brain morphometry. WM, GMV, and cortical thickness are known to decline as an individual grows older (Lemaitre et al., 2012; Salthouse and Babcock, 1991), while ICV is commonly used as a covariate to account for differences in gray matter due to head and body size (Hansen et al., 2015). Cortical parcellation was used to extract estimates of gray matter volume (GMV) and cortical thickness in cortical regions defined by the Desikan atlas (Desikan et al., 2006) and cortical GMV as a whole. GMV and cortical thickness values for each cortical region were then exported into Statistical Package for Social Sciences (SPSS version 24) for analysis with behavioral and brain activation measures. Covariate-adjusted partial correlations were completed to test the associations of total cortical GMV with 2-back accuracy. Then, covariate-adjusted partial correlations were examined between GMV and cortical thickness in specific brain regions and 2-back accuracy (see Supplementary Table 1 for full list of regions). Given the large number of cortical regions in the Desikan atlas (68), a two-tailed false discovery rate correction (Benjamini and Hochberg, 1995) of $q = .05$ was implemented to reduce inflation of type I error rate. The primary reason for including parcellation analyses in addition to voxelwise analyses was for these regions inclusion in integrative regression models (described in greater detail below). Additionally, to parse the degree to which structural associations with 2-back accuracy were specific to WM (as opposed to other processes involved in the 2-back task), accuracy on the 0-back visuomotor control task was also examined in relation to GMV and cortical thickness in the 68 Desikan atlas regions using partial correlation analyses analogous to those described above. Subsequently, cortical surface voxelwise analysis was used to assess the relationship of GMV with 2-back accuracy using a voxel-by-voxel following the procedure described by Fischl and Dale (Dale et al., 1999; Fischl et al., 1999a). This was done entirely in FreeSurfer (Fischl, 2012) with the final output being a brain map of correlations between GMV and 2-back accuracy and a table of all clusters of correlation between GMV and 2-Back accuracy. The same voxelwise analyses were also conducted for cortical thickness. Cortical surface voxelwise analysis allows the statistical comparison and visualization of volume in

analogous regions across subjects using a common space based on the 2D surface of the brain rather than a 3D template of the brain, which is considered to be superior given inherent differences in brain topography from subject to subject. Clusterwise correction for multiple comparisons in both cases was conducted using Monte Carlo simulations (Hagler et al., 2006). Specifically, the data are tested against a null distribution of maximum cluster size with an initial cluster-forming threshold of $p < .001$, which yields clusters corrected for multiple comparisons based on the total number of comparisons on the surface. Using this method, regions in which GMV/thickness were associated with 2-back accuracy at a cluster-corrected $p<.05$ were determined.

Integration of Structural and Functional MRI Data—To determine which of the regions in the previous analyses were uniquely associated with 2-back accuracy (i.e., beyond shared variance among regions) hierarchical multiple regression was applied to the regions surviving FDR correction in the above partial correlation analyses. As a part of this analysis, bivariate correlations were conducted to explore multicollinearity between the 3 sets of regions in which GMV was bilaterally related to 2-back accuracy (i.e., lateral orbitofrontal cortex, cuneus, temporal pole), revealing substantial associations (rs > .67) between all bilateral sets (see Supplementary Table 3). As a result, these regions were consolidated (i.e., summed) in the final regression analyses to avoid multicollinearity in subsequent multiple regression models. The same process was completed with the 18 regions in which 2-back BOLD activation (relative to 0-back) was bilaterally associated with 2-back accuracy, revealing significant association between bilateral activations as well. These regions were consolidated as well using the mean of the activation in the two regions. Then, in multiple regression models, age and ICV were entered into the model first and activation in the regions associated with 2-back accuracy in partial correlation analyses were entered one-by-one starting with the largest and progressing to the lowest effect size. Those that significantly increased the variance explained by the model (i.e., had a significant R^2 change score, $p<.05$) were retained in the model. GMV in the regions associated in structural MRI partial correlations analyses with 2-back accuracy were then entered one-by-one starting with the largest effect size and progressing to the lowest effect size. Those which improved the variance explained by the model when added were retained in the model. Next, cortical thickness in the regions associated with 2-back accuracy in partial correlation analyses were entered one-by-one starting with the largest effect size and progressing to the lowest effect size. This resulted in a model which tested the effects of regional GMV and cortical thickness as predictors of 2-back accuracy above and beyond covariates and functional correlates of WM. Additionally, the model was tested with age removed to ensure final results were not an artifact of the decision to covary for age (Supplemental Table 9). Last, the associations of brain structure and function was directly investigated using Pearson's correlations to examine the association of regional brain activity with GMV and cortical thickness in the same region.

Supplementary Material

Refer to Web version on PubMed Central for supplementary material.

ACKNOWLEDGEMENTS

REFERENCES

Almeida LG, Ricardo-Garcell J, Prado H, Barajas L, Fernández-Bouzas A, Ávila D, Martínez RB, 2010 Reduced right frontal cortical thickness in children, adolescents and adults with ADHD and its correlation to clinical variables: A cross-sectional study. J. Psychiatr. Res 44, 1214–1223. doi: 10.1016/j.jpsychires.2010.04.026 [PubMed: 20510424]

Andrews-Hanna JR, Reidler JS, Sepulcre J, Poulin R, Buckner RL, 2010 Functional-Anatomic Fractionation of the Brain's Default Network. Neuron 65, 550–562. doi:10.1016/j.neuron. 2010.02.005 [PubMed: 20188659]

Benjamini Y, Hochberg Y, 1995 Controlling the false discovery rate: A practical and powerful approach to multiple testing. J. R. Stat. Soc. Ser. B 57, 289–300. doi:10.2307/2346101

Bickel WK, Yi R, Landes RD, Hill PF, Baxter C, 2011 Remember the future: working memory training decreases delay discounting among stimulant addicts. Biol. Psychiatry 69, 260–5. doi: 10.1016/j.biopsych.2010.08.017 [PubMed: 20965498]

Bjork JM, Momenan R, Hommer DW, 2009 Delay Discounting Correlates with Proportional Lateral Frontal Cortex Volumes. Biol. Psychiatry 65, 710–713. doi:10.1016/j.biopsych.2008.11.023 [PubMed: 19121516]

Bobholz JA, Rao SM, 2003 Cognitive dysfunction in multiple sclerosis: a review of recent developments. Curr. Opin. Neurol 16, 283–288. doi:10.1097/01.wco.0000073928.19076.84 [PubMed: 12858063]

Buckner RL, Andrews-Hanna JR, Schacter DL, 2008 The brain's default network: Anatomy, function, and relevance to disease. Ann. N. Y. Acad. Sci doi:10.1196/annals.1440.011

Burgess GC, Gray JR, Conway ARA, Braver TS, 2011 Neural mechanisms of interference control underlie the relationships between Fluid intelligence and working memory span. J. Exp. Psychol. Gen 140, 674–92. doi:10.1037/a0024695.Neural [PubMed: 21787103]

Cabeza R, Anderson ND, Locantore JK, McIntosh AR, 2002 Aging Gracefully: Compensatory Brain Activity in High-Performing Older Adults. Neuroimage 17, 1394–1402. doi:10.1006/nimg. 2002.1280 [PubMed: 12414279]

Chein JM, Moore AB, Conway ARA, 2011 Domain-general mechanisms of complex working memory span. Neuroimage 54, 550–559. doi:10.1016/j.neuroimage.2010.07.067 [PubMed: 20691275]

Cox RW, 1996 AFNI: software for analysis and visualization of functional magnetic resonance neuroimages. Comput Biomed Res 29, 162–173. [PubMed: 8812068]

Dale AM, Fischl B, Sereno MI, 1999 Cortical surface-based analysis. I. Segmentation and surface reconstruction. Neuroimage 9, 179–194. doi:10.1006/nimg.1998.0395 [PubMed: 9931268]

Desikan RS, Segonne F, Fischl B, Quinn BT, Dickerson BC, Blacker D, Buckner RL, Dale AM, Maguire RP, Hyman BT, Albert MS, Killiany RJ, 2006 An automated labeling system for subdividing the human cerebral cortex on MRI scans into gyral based regions of interest. Neuroimage 31, 968–980. doi:10.1016/j.neuroimage.2006.01.021 [PubMed: 16530430]

Durazzo TC, Tosun D, Buckley S, Gazdzinski S, Mon A, Fryer SL, Meyerhoff DJ, 2011 Cortical thickness, surface area, and volume of the brain reward system in alcohol dependence: Relationships to relapse and extended abstinence. Alcohol. Clin. Exp. Res 35, 1187–1200. doi: 10.1111/j.1530-0277.2011.01452.x [PubMed: 21410483]

Fischl B, 2012 FreeSurfer. Neuroimage doi:10.1016/j.neuroimage.2012.01.021

Fischl B, Liu A, Dale AM, 2001 Automated manifold surgery: Constructing geometrically accurate and topologically correct models of the human cerebral cortex. IEEE Trans. Med. Imaging 20, 70–80. doi:10.1109/42.906426 [PubMed: 11293693]

Fischl B, Sereno MI, Dale AM, 1999a Cortical Surface-Based Analysis: II: Inflation, Flattening, and a Surface-Based Coordinate System. Neuroimage 9, 195–207. doi:10.1006/nimg.1998.0396 [PubMed: 9931269]

Fischl B, Sereno MI, Tootell RBH, Dale AM, 1999b High-resolution intersubject averaging and a coordinate system for the cortical surface. Hum. Brain Mapp 8, 272–284. doi:10.1002/(SICI)1097-0193(1999)8:4<272::AID-HBM10>3.0.CO;2-4 [PubMed: 10619420]

Glasser MF, Sotiropoulos SN, Wilson JA, Coalson TS, Fischl B, Andersson JL, Xu J, Jbabdi S, Webster M, Polimeni JR, Van Essen DC, Jenkinson M, 2013 The minimal preprocessing pipelines for the Human Connectome Project. Neuroimage 80, 105–124. doi:10.1016/j.neuroimage.2013.04.127 [PubMed: 23668970]

Goldman-Rakic PS, 1994 Working memory dysfunction in schizophrenia. J. Neuropsychiatry Clin. Neurosci 6, 348–357. doi:10.1176/jnp.6.4.348 [PubMed: 7841806]

Hagler DJ, Saygin AP, Sereno MI, 2006 Smoothing and cluster thresholding for cortical surface-based group analysis of fMRI data. Neuroimage 33, 1093–1103. doi:10.1016/j.neuroimage.2006.07.036 [PubMed: 17011792]

Haldane M, Cunningham G, Androutsos C, Frangou S, 2008 Structural brain correlates of response inhibition in Bipolar Disorder I. J. Psychopharmacol 22, 138–143. doi:10.1177/0269881107082955 [PubMed: 18308812]

Hansen TI, Brezova V, Eikenes L, Håberg A, Vangberg XTR, 2015 How does the accuracy of intracranial volume measurements affect normalized brain volumes? sample size estimates based on 966 subjects from the HUNT MRI cohort. Am. J. Neuroradiol 36, 1450–1456. doi:10.3174/ajnr.A4299 [PubMed: 25857759]

Herting MM, Gautam P, Spielberg JM, Dahl RE, Sowell ER, 2015 A longitudinal study: Changes in cortical thickness and surface area during pubertal maturation. PLoS One 10. doi:10.1371/journal.pone.0119774

Jacola LM, Willard VW, Ashford JM, Ogg RJ, Scoggins MA, Jones MM, Wu S, Conklin HM, 2014 Clinical utility of the N-back task in functional neuroimaging studies of working memory. J. Clin. Exp. Neuropsychol 36, 875–886. doi:10.1080/13803395.2014.953039 [PubMed: 25252868]

Jaeggi SM, Buschkuehl M, Perrig WJ, Meier B, 2010 The concurrent validity of the N-back task as a working memory measure. Memory 18, 394–412. doi:10.1080/09658211003702171 [PubMed: 20408039]

Kane MJ, Conway ARA, Miura TK, Colflesh GJH, 2007 Working Memory, Attention Control, and the N-Back Task: A Question of Construct Validity. J. Exp. Psychol. Learn. Mem. Cogn 33, 615–622. doi:10.1037/0278-7393.33.3.615 [PubMed: 17470009]

Lemaitre H, Goldman AL, Sambataro F, Verchinski BA, Meyer-Lindenberg A, Weinberger DR, Mattay VS, 2012 Normal age-related brain morphometric changes: Nonuniformity across cortical thickness, surface area and gray matter volume? Neurobiol. Aging 33. doi:10.1016/j.neurobiolaging.2010.07.013

Marcus DS, Harms MP, Snyder AZ, Jenkinson M, Wilson JA, Glasser MF, Barch DM, Archie KA, Burgess GC, Ramaratnam M, Hodge M, Horton W, Herrick R, Olsen T, McKay M, House M, Hileman M, Reid E, Harwell J, Coalson T, Schindler J, Elam JS, Curtiss SW, Van Essen DC, 2013 Human Connectome Project informatics: Quality control, database services, and data visualization. Neuroimage 80, 202–219. doi:10.1016/j.neuroimage.2013.05.077 [PubMed: 23707591]

Martinussen R, Hayden J, Hogg-Johnson S, Tannock R, 2005 A meta-analysis of working memory impairments in children with attention-deficit/hyperactivity disorder. J. Am. Acad. Child Adolesc. Psychiatry 44, 377–84. doi:10.1097/01.chi.0000153228.72591.73 [PubMed: 15782085]

McKiernan KA, Kaufman JN, Kucera-Thompson J, Binder JR, 2003 A parametric manipulation of factors affecting task-induced deactivation in functional neuroimaging. J. Cogn. Neurosci 15, 394–408. doi:10.1162/089892903321593117 [PubMed: 12729491]

Miller EK, 2000 The prefrontal cortex and cognitive control. Nat. Rev. Neurosci 1, 59–65. doi:10.1038/35036228 [PubMed: 11252769]

Miller KM, Price CC, Okun MS, Montijo H, Bowers D, 2009 Is the N-back task a valid neuropsychological measure for assessing working memory? Arch. Clin. Neuropsychol 24, 711–717. doi:10.1093/arclin/acp063 [PubMed: 19767297]

Niendam TA, Laird AR, Ray KL, Dean YM, Glahn DC, Carter CS, 2012 Meta-analytic evidence for a superordinate cognitive control network subserving diverse executive functions. Cogn Affect Behav Neurosci 12, 241–268. doi:10.3758/s13415-011-0083-5 [PubMed: 22282036]

Nissim NR, O'Shea AM, Bryant V, Porges EC, Cohen R, Woods AJ, 2017 Frontal structural neural correlates of working memory performance in older adults. Front. Aging Neurosci 8. doi:10.3389/fnagi.2016.00328

Nyberg L, Dahlin E, Stigsdotter Neely A, Backman L, 2009 Neural correlates of variable working memory load across adult age and skill: Dissociative patterns within the frontoparietal network: Cognition and Neurosciences. Scand. J. Psychol 50, 41–46. doi:10.1111/j.1467-9450.2008.00678.x [PubMed: 18705668]

Oberauer K, Süß H-M, Wilhelm O, Sander N, 2012 Individual differences in working memory capacity and reasoning ability, in: Conway ARA, Jarrold C, Kane MJ, Miyake A, Towse JN (Eds.), Variation in Working Memory Oxford University Press, New York, pp. 49–75. doi:10.1093/acprof:oso/9780195168648.001.0001

Olesen PJ, Westerberg H, Klingberg T, 2004 Increased prefrontal and parietal activity after training of working memory. Nat. Neurosci 7, 75–79. doi:10.1038/nn1165 [PubMed: 14699419]

Osaka N, Osaka M, Kondo H, Morishita M, Fukuyama H, Shibasaki H, 2004 The neural basis of executive function in working memory: An fMRI study based on individual differences. Neuroimage 21, 623–631. doi:10.1016/j.neuroimage.2003.09.069 [PubMed: 14980565]

Owen AM, McMillan KM, Laird AR, Bullmore E, 2005 N-back working memory paradigm: A meta-analysis of normative functional neuroimaging studies, in: Human Brain Mapping pp. 46–59. doi:10.1002/hbm.20131 [PubMed: 15846822]

Raine A, Lencz T, Bihrle S, LaCasse L, Colletti P, 2000 Reduced prefrontal gray matter volume and reduced autonomic activity in antisocial personality disorder. Arch. Gen. Psychiatry 57, 119–27–10.1001/archpsyc.57.2.119 [PubMed: 10665614]

Rao SM, Grafman J, DiGiulio D, Mittenberg W, 1993 Memory dysfunction in multiple sclerosis: Its relation to working memory, semantic encoding, and implicit learning. Neuropsychology 7, 364–374. doi:10.1037/0894-4105.7.3.364

Redick TS, Lindsey DRB, 2013 Complex span and n-back measures of working memory: A meta-analysis. Psychon. Bull. Rev 20, 1102–1113. doi:10.3758/s13423-013-0453-9 [PubMed: 23733330]

Rorden C, 2007 Dcm2nii to NIFTI converter

Salat DH, Kaye JA, Janowsky JS, 2002 Greater Orbital Prefrontal Volume Selectively Predicts Worse Working Memory Performance in Older Adults. Cereb. Cortex 12, 494–505. doi:10.1093/cercor/12.5.494 [PubMed: 11950767]

Salthouse TA, Babcock RL, 1991 Decomposing adult age differences in working memory. Dev. Psychol 27, 763–776. doi:10.1037/0012-1649.27.5.763

Silver H, Feldman P, Bilker W, Gur RC, 2003 Working memory deficit as a core neuropsychological dysfunction in schizophrenia. Am. J. Psychiatry 160, 1809–1816. doi:10.1176/appi.ajp.160.10.1809 [PubMed: 14514495]

Smith EE, Jonides J, 1997 Working memory: a view from neuroimaging. Cogn. Psychol 33, 5–42. doi:10.1006/cogp.1997.0658 [PubMed: 9212720]

Squeglia LM, McKenna BS, Jacobus J, Castro N, Sorg SF, Tapert SF, 2013 BOLD response to working memory not related to cortical thickness during early adolescence. Brain Res 1537, 59–68. doi:10.1016/j.brainres.2013.08.053 [PubMed: 24012876]

Sweet LH, Paskavitz JF, Haley AP, Gunstad JJ, Mulligan RC, Nyalakanti PK, Cohen RA, 2008 Imaging phonological similarity effects on verbal working memory. Neuropsychologia 46, 1114–1123. doi:10.1016/j.neuropsychologia.2007.10.022 [PubMed: 18155074]

Takeuchi H, Taki Y, Sassa Y, Hashizume H, Sekiguchi A, Fukushima A, Kawashima R, 2011 Working memory training using mental calculation impacts regional gray matter of the frontal and parietal regions. PLoS One 6. doi:10.1371/journal.pone.0023175

Unsworth N, Miller JD, Lakey CE, Young DL, Meeks JT, Campbell WK, Goodie AS, 2009 Exploring the Relations Among Executive Functions, Fluid Intelligence, and Personality. J. Individ. Differ 30, 194–200. doi:10.1027/1614-0001.30.4.194

Van Essen D, Ugurbil K, Auerbach E, Barch D, Behrens T, Bucholz R, Chang A, Chen L, Corbetta M, Curtiss S, Della Penna S, Feinberg D, Glasser M, Harel N, Heath A, Larson-Prior L, Marcus D, Michalareas G, Moeller S, Oostenveld R, Petersen S, Prior F, Schlaggar B, Smith S, Snyder A, Xu J, Yacoub E, 2013 The Human Connectome Project : A data acquisition perspective. Neuroimage 62, 2222–2231. doi:10.1016/j.neuroimage.2012.02.018.The

Van Essen DC, Smith SM, Barch DM, Behrens TEJ, Yacoub E, Ugurbil K, 2013 The WU-Minn Human Connectome Project: An overview. Neuroimage 80, 62–79. doi:10.1016/j.neuroimage. 2013.05.041 [PubMed: 23684880]

Vanni S, Tanskanen T, Seppä M, Uutela K, Hari R, 2001 Coinciding early activation of the human primary visual cortex and anteromedial cuneus. Proc. Natl. Acad. Sci. U. S. A 98, 2776–80. doi: 10.1073/pnas.041600898 [PubMed: 11226316]

Vijayakumar N, Allen NB, Youssef G, Dennison M, Yücel M, Simmons JG, Whittle S, 2016 Brain development during adolescence: A mixed-longitudinal investigation of cortical thickness, surface area, and volume. Hum. Brain Mapp 37, 2027–2038. doi:10.1002/hbm.23154 [PubMed: 26946457]

Wager TD, Smith EE, 2003 Neuroimaging studies of working memory: a meta-analysis. Cogn. Affect. Behav. Neurosci 3, 255–274. doi:10.3758/CABN.3.4.255 [PubMed: 15040547]

Yang Y, Raine A, Lencz T, Bihrle S, LaCasse L, Colletti P, 2005 Volume reduction in prefrontal gray matter in unsuccessful criminal psychopaths. Biol. Psychiatry 57, 1103–1108. doi:10.1016/j.biopsych.2005.01.021 [PubMed: 15866549]

Yeo BT, Krienen FM, Eickhoff SB, Yaakub SN, Fox PT, Buckner RL, Asplund CL, Chee MWL, 2015 Functional specialization and flexibility in human association cortex. Cereb. Cortex 25, 3654–3672. doi:10.1093/cercor/bhu217 [PubMed: 25249407]
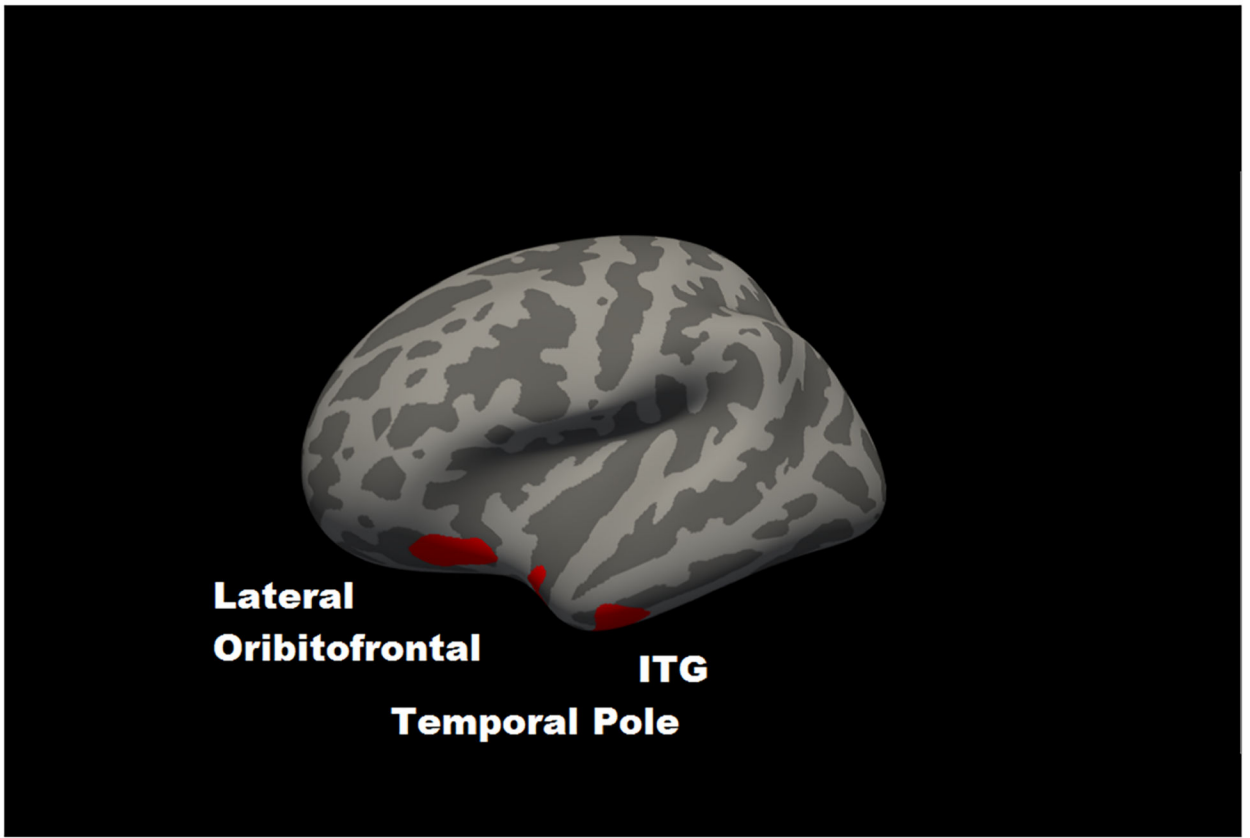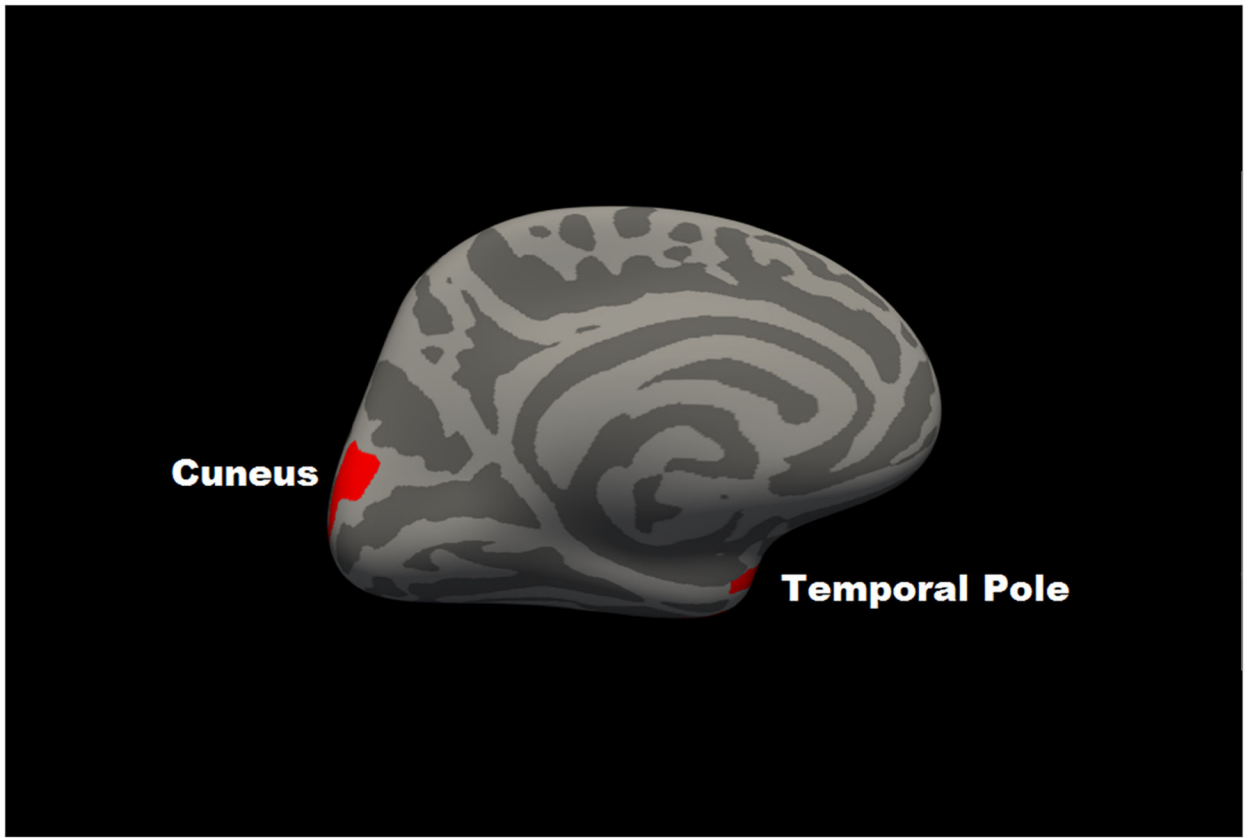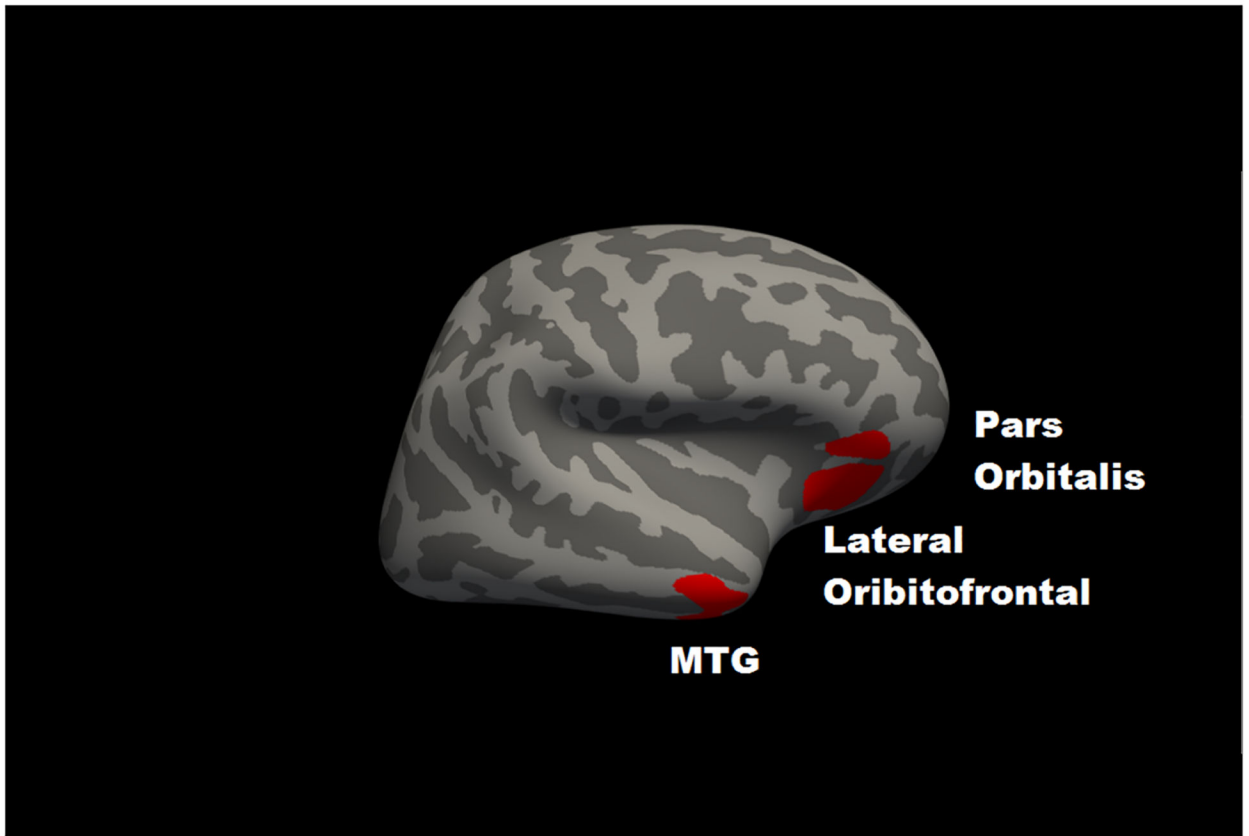
Figure 1. Significant voxelwise correlations between gray matter volume and 2-back accuracy at cluster-corrected threshold of *p* < .05.
Panel A shows left hemisphere lateral view; Panel B shows a left hemisphere medial view;

Panel C shows a right hemisphere lateral view. ITG = inferior temporal gyrus; MTG = middle temporal gyrus.
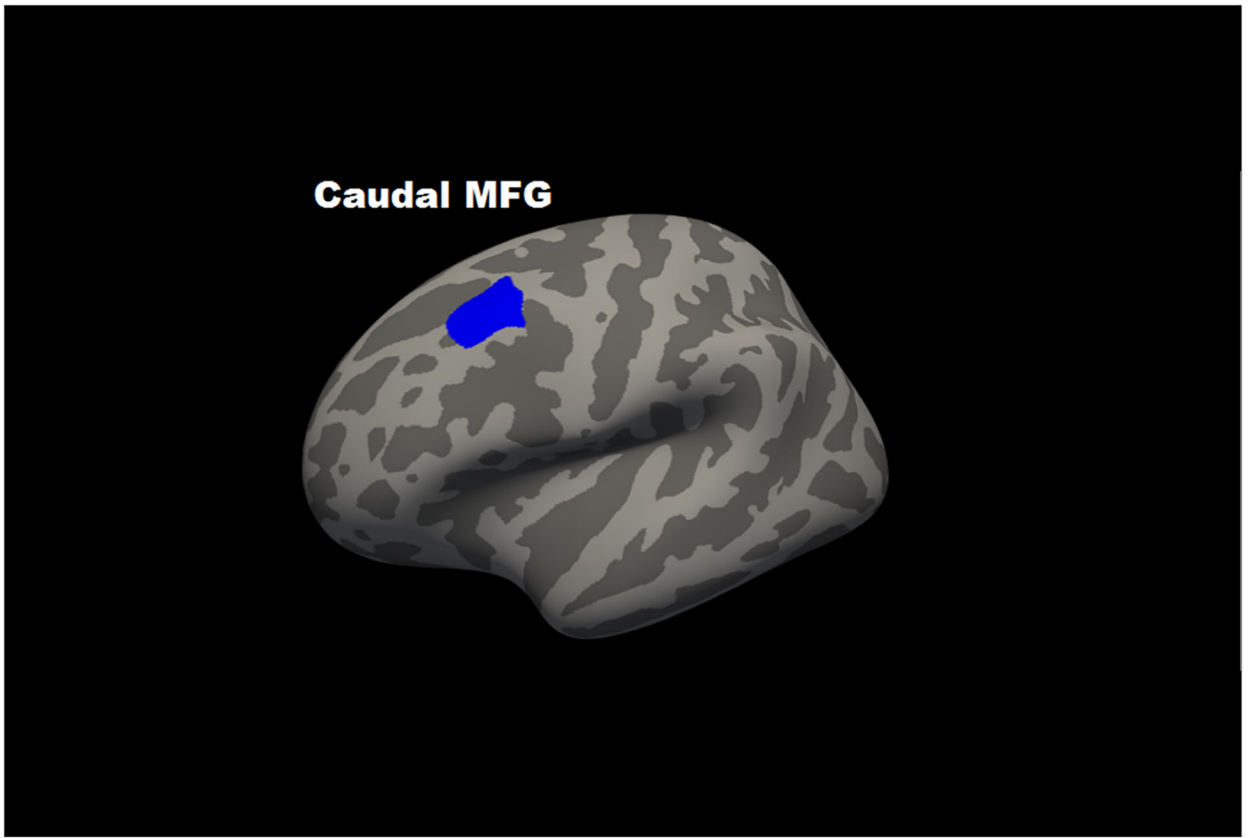
Caudal MFG

Figure 2. Map of significant voxelwise correlations between cortical thickness and 2-back accuracy at cluster-corrected threshold of $p < .05$.
Panel A shows left hemisphere lateral view; Panel B shows a right hemisphere medial view.

Blue represents regions in which corticial thickness was negatively associated with 2-back accuracy; red represents regions in which cortical thickness was positively associated with 2-back accuracy.
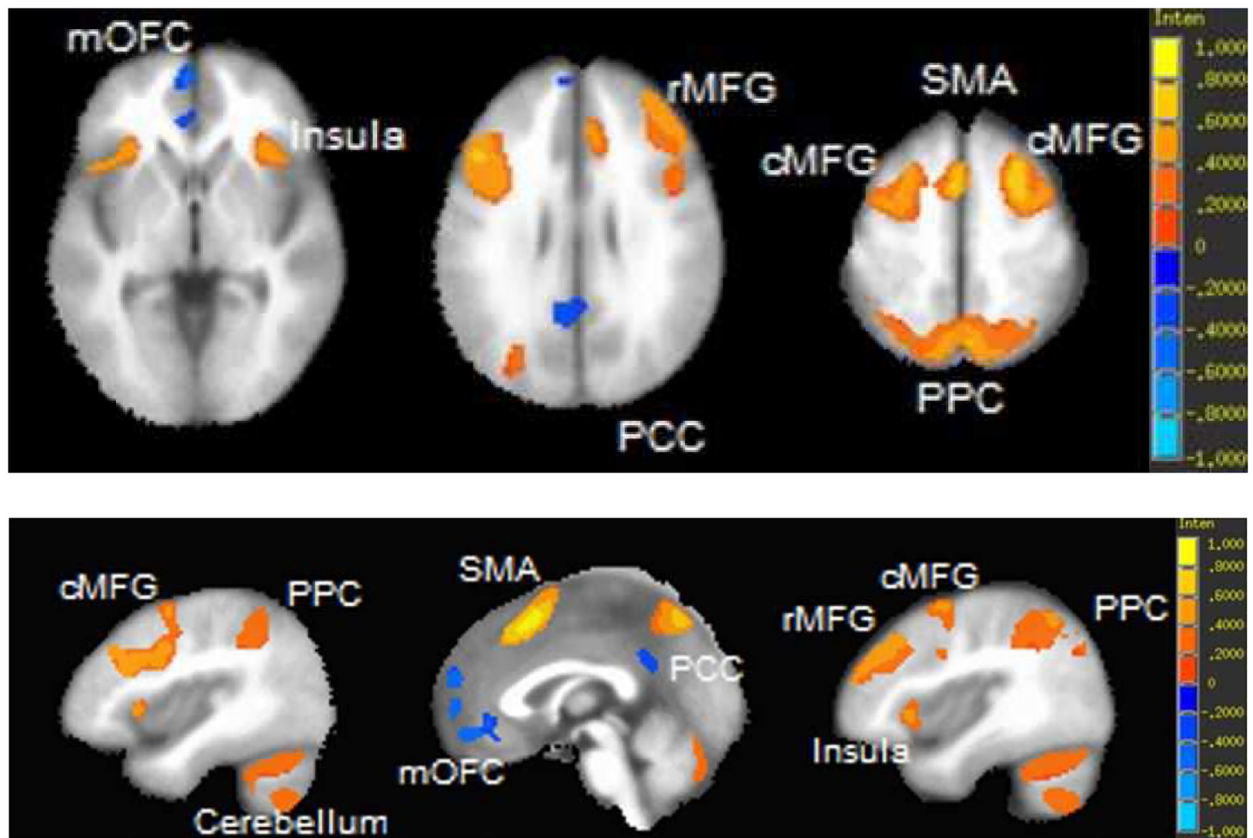
Figure 3. Voxelwise partial correlation of 2-back accuracy and activation during 2-back (relative to 0-back) controlling for age at a threshold of *p* < 1E-11 and cluster threshold of 200.
Panel A = axial view, z coordinates left to right: 13 28 43. Panel B = sagittal view, x coordinates left to right: -20 0 20. Both panels include the scale of activaitons in percent signal change; maximum and minimum of scale (1 and -1): β = ±20.15, *t* = ±12.8. mOFC = medial orbitofrontal cortex, rMFG = rostral middle frontal gyrus; PCC = posterior cingulate cortex; SMA = supplementary motor area; cMFG = caudal middle frontal gyrus; PPC = posterior parietal cortex.

Table 1.
Working Memory Performance and Brain Morphometry.

Panel A shows partial correlations of a gray matter volume in segmented regions (based on Desikan atlas) with 2-back accuracy controlling for age and total intracranial volume. Only regions with significant p-values after FDR are included (q < .05). Panel B shows a summary of clusters in voxelwise analysis of gray matter volume. Coordinates of peak significance provided in Montreal Neurological Institute space (X Y Z). CWP = cluster-wise p-value.

A	Hemi	Region	r
	L	Lateral Orbitofrontal	.120
	L	Cuneus	.118
	R	Middle Temporal Gyrus	.112
	R	Lateral Orbitofrontal	.109
	R	Pars Orbitalis	.107
	L	Inferior Temporal Gyrus	.102
	L	Rostral Anterior Cingulate	.096
	L	Lateral Occipital	.093
	L	Pericalcarine Fissure	.090
	L	Entorhinal Cortex	.090
	L	Insula	.080
	R	Cuneus	.080
	L	Temporal Pole	.079
	R	Temporal Pole	.079

B	Left Hemisphere Volume	Size (mm3)	X	Y	Z	CWP
	Cuneus	586	−4	−84	21	.0002
	Lateral Orbitofrontal Cortex	459	−29	19	−19	.0002
	Inferior Temporal Gyrus	451	−46	−8	−37	.0002
	Temporal Pole	250	−31	4	−32	.0103
	Right Hemisphere Volume	**Size (mm^3)**	**X**	**Y**	**Z**	**CWP**
	Middle Temporal Gyrus	713	48	2	−33	.0002
	Lateral Orbitofrontal Cortex	560	38	28	−17	.0036
	Pars Orbitalis	294	47	38	−13	.0002

Table 2.
Associations between BOLD signal and N-Back performance.

Panel A shows partial correlations of brain activation during 2-back (relative to 0-back) in Desikan atlas regions with significance level $p < 5.00E-5$ (all regions and raw p-values are in Supplementary Table 3). Panel B shows clusters of activation during 2-back (relative to 0-back) at $p < 1E-11$ with a minimum cluster size of 200 voxels. Peak coordinates are in MNI space.

A	Hemi	Region	r
	R	Caudal Middle Frontal Gyrus	0.315
	L	Superior Parietal Lobule	0.297
	R	Superior Parietal Lobule	0.290
	R	Rostral Middle Frontal Gyrus	0.276
	L	Caudal Middle Frontal Gyrus	0.272
	L	Medial Orbitofrontal Cortex	−0.263
	L	Frontal Pole	−0.248
	R	Medial Orbitofrontal Cortex	−0.228
	L	Rostral Middle Frontal Gyrus	0.226
	R	Inferior Parietal Lobule	0.220
	L	Pars Opercularis	0.198
	L	Lingual Gyrus	0.171
	L	Lateral Occipital Cortex	0.169
	L	Rostral Anterior Cingulate	−0.166
	R	Pars Opercularis	0.164
	R	Lingual Gyrus	0.156
	R	Superior Frontal Gyrus	0.148
	R	Frontal Pole	−0.140
	R	Rostral Anterior Cingulate	−0.132
	L	Inferior Parietal Lobule	0.126

B	Hemi	Region Name	Size in Voxels	X	Y	Z
	B	Bilateral Posterior Parietal	5759	2	−68	50
	R	Cerebellum	3097	−6	−80	−22
	L	Caudal Middle Frontal Gyrus	2153	−50	14	32
	R	Rostral Middle Frontal Gyrus	1510	44	36	32
	B	Supplementary Motor Area	1361	0	16	50
	R	Caudal Middle Frontal Gyrus	1319	28	14	60
	L	Medial Orbitofrontal Cortex	521	−2	58	4
	L	Cerebellum	339	−38	−70	−52
	L	Insula	338	−30	26	0
	R	Insula	324	34	26	0
	L	Rostral Middle Frontal Gyrus	243	−30	58	12
	B	Posterior Cingulate Cortex	229	−8	−52	30
	L	Medial Orbitofrontal Cortex	227	−2	54	−12

Table 3.

Regression of cortical parcellation regions of interest as predictors of 2-back accuracy.

β_e represents standardized regression coefficients at the time of entry to the model. p_e represents the alpha of the F statistic associated with R^2 at the time of entry into the model. β_f represents the regression coefficients in the final model and p_f represents the alpha value of the regression coefficient in the final model. GMV = gray matter volume; THICK = cortical thickness; MFG = middle frontal gyrus; OFC = orbitofrontal cortex.

	Independent Variables	β_e	p_e	R^2	R^2	β_f	p_f
Covariates	Age	−.153	<.001	.023	.023	−.048	.093
	Total Intracranial Volume	.221	<.001	.070	.047	.016	.706
BOLD Activation	Bilateral Caudal MFG	.298	<.001	.156	.086	.254	<.001
	Bilateral Superior Parietal Lobule	.151	<.001	.168	.011	.278	<.001
	Bilateral Medial OFC	−.198	<.001	.203	.036	−.062	.154
	Bilateral Frontal Pole	−.117	.004	.209	.006	−.065	.112
	Bilateral Inferior Parietal Lobule	−.117	.029	.213	.004	−.126	.019
	Bilateral Pars Opercularis	−.091	.050	.216	.003	−.048	.356
	Bilateral Transverse Temporal	−.074	.041	.219	.003	−.066	.110
	Bilateral Fusiform Gyrus	.137	<.001	.228	.009	.155	<.001
	Bilateral Supramarginal Gyrus	−.140	.004	.234	.006	−.110	.021
	Bilateral Isthmus of Cingulate	−.116	.002	.241	.007	−.104	.006
Structural Indices	Bilateral Lateral OFC GMV	.157	<.001	.252	.011	.157	<.001
	Bilateral Cuneus GMV	.076	.027	.255	.003	.070	.042
	Bilateral Caudal MFG THICK	−.094	.001	.263	.008	−.094	.001

Table 4.

Significant Pearson correlations between regional BOLD activation during the 2-back task and corresponding gray matter volume at a FDR correction of $q = .05$. *indicates that BOLD signal in a region was significantly associated with 2-back accuracy; #indicates that gray matter volume in a region was associated with 2-back accuracy.

Hemi	Region	*r*	*P*
R	Superior Parietal Lobule*	.151	7E-7
R	Inferior Parietal Lobule*	.118	1E-4
L	Superior Parietal Lobule*	.114	2E-4
L	Medial Orbitofrontal Cortex*	−.111	2E-4
R	Temporal Pole#	−.104	6E-4
R	Rostral Middle Frontal Gyrus*	.102	8E-4
R	Medial Orbitofrontal Cortex*	−.093	.002
R	Caudal Anterior Cingulate	.091	.003
L	Middle Temporal Gyrus	−.086	.005
R	Precuneus	.084	.006
R	Supramarginal Gyrus*	.083	.007
L	Entorhinal Cortex#	−.082	.007

Table 5.

Demographic characteristics of final sample ($N = 1064$)

DEMOGRAPHIC CHARECTERISTIC	M (SD) or %
Sex	
Male	46
Female	54
Age	28.80 (3.68)
Race	
White or Caucasian	75
Black or African American	14.5
Asian American, Native Hawaiian, or other Pacific Islander	6.0
Native American	.2
More than one race	2.6
Not sure or unknown	1.7
Ethnicity	
Hispanic or Latino	8.7
Not Hispanic or Latino	90
Not sure or unknown	1.2
Income	
$1,000–$9,999/year	6.9
$10,000–$19,999/year	7.5
$20,000–$29,999/year	12.9
$30,000–$39,999/year	11.8
$40,000–$49,999/year	10.3
$50,000–$74,999/year	21.1
$75,000–$99,999/year	13.6
$100,000–$149,999/year	15.7
Years of Education	14.95 (1.78)